Available online at www.sciencedirect.com
ScienceDirect
Journal of Magnetic Resonance 191 (2008) 259–266
JMR Journal of Magnetic Resonance
www.elsevier.com/locate/jmr

Chemical shift anisotropy edited complete unraveling of overlapped ^{1}H NMR spectra of enantiomers: Application to small chiral molecules

Uday Ramesh Prabhu [a], Bikash Baishya [a], N. Suryaprakash [b,*]

[a] Solid State and Structural Chemistry Unit, Indian Institute of Science, SIF, Bangalore, Karnataka 560012, India
[b] NMR Research Centre, Indian Institute of Science, SIF, Bangalore, Karnataka 560012, India

Received 16 September 2007; revised 23 December 2007
Available online 5 January 2008

Abstract

The differential values of NMR spectral parameters like chemical shift anisotropies, dipolar couplings and quadrupolar couplings of enantiomers in chiral liquid crystalline media are employed not only for their visualization but also for their quantification. Large differences in chemical shift anisotropies and the quadrupolar couplings between the enantiomers enable the use of ^{13}C and extensive ^{2}H NMR detection for such a purpose. In spite of high magnetic moment, high sensitivity and abundant presence of protons in all the chiral molecules, ^{1}H detection is not routinely employed due to severe overlap of unresolved transitions arising from short and long distance couplings. Furthermore, the doubling of the spectra from two enantiomers and their indistinguishable overlap due to negligible difference in chemical shift anisotropies hampers their discrimination. The present study demonstrates the use of proton chemical shift anisotropy as an exclusive parameter for such a discrimination. The method employs the non-selective excitation of homonuclear *N*th quantum coherence of *N* coupled protons. The simultaneous flipping of all the coupled spins results in a single transition in the multiple quantum dimension at the cumulative sum of their anisotropic chemical shifts for each enantiomer, with the measurable difference between them, resulting in their complete unraveling.

Keywords: Multiple quantum; Chemical shift anisotropy; Chiral discrimination

1. Introduction

NMR spectroscopic visualization of optical enantiomers is extensively practiced using the weakly aligned chiral lyotropic liquid crystalline media [1–3]. The difference in the orientational property of the enantiomers has been exploited for their visualization and to determine their excess. The elements of the Saupe order matrix of the enantiomers differ by a small magnitude and are of the order of 10^{-3} to 10^{-5} [4]. However, its effect on the anisotropic NMR spectral parameters like chemical shift anisotropies ($\Delta\sigma_i$), dipolar couplings (D_{ij}) and quadrupolar couplings (Q_i) are significant as far as the visualization of enantiomers is concerned. In the case of proton detection, the magnitudes of chemical shift anisotropies and their differential values between the enantiomers are not significant and many a time results in an indistinguishable overlap of the spectra. Thus the dipolar couplings among the protons are the obvious choice for their visualization. However, in chiral molecules with large number of interacting protons there is a significant loss of resolution due to several short and long distance dipolar couplings and the doubling of transitions from the two enantiomers. This severely hampers the complete unraveling of the spectra and their analyses. Nevertheless, the strengths of the dipolar couplings in chiral media are not large unlike in the strongly orienting thermotropic liquid crystals and in favorable cases permit the first order analyses of the spectra similar to that of liquid state spectra. But the challenging task of both unraveling of the spectra and achieving high resolution always persists. Hence the majority of NMR investiga-

* Corresponding author. Fax: +91 80 2360 1550.
E-mail address: nsp@sif.iisc.ernet.in (N. Suryaprakash).

1090-7807/$ - see front matter © 2008 Elsevier Inc. All rights reserved.
doi:10.1016/j.jmr.2007.12.019

tions of enantiomeric differentiation have focused on ^{2}H NMR [5–11], taking advantage of the relatively large strengths of the quadrupole couplings compared to chemical shift anisotropies and dipolar couplings. The recent study also discusses the use of homo and heteronuclear two-dimensional methods to analyse a mixture of deuterated unlike and like stereo isomers [12]. There are also studies using ^{13}C [13,14] and ^{19}F [15,16]. In spite of severe overlap of the transitions, the proton detection is advantageous because of; (a) its high magnetic moment, (b) high natural abundance and (c) abundant presence in all the chiral organic molecules. Thus there are continuous efforts on methodological developments reported in the literature for discrimination of enantiomers, viz., selective refocusing (SERF) experiment [17] based on the selective excitation [18] used in liquid state studies to determine the scalar couplings, combined variable angle with selective refocusing [19], two-dimensional correlation [20], heteronuclear selective refocusing [21], *J*-resolved experiment with BIRD sequence [22]. Each of these methods has its own advantages.

In our recent study on heteronuclear spin systems, we have demonstrated the selective detection of single quantum (SQ) coherence based on the spin state of the heteronuclei using highest order of homonuclear multiple quantum (MQ) coherence [23]. The method simplified the analyses of the complex NMR spectra of strongly dipolar coupled spins and removed the redundancy in the number of observable SQ transitions as far as the determination of homonuclear couplings is concerned. We extended this methodology for the weakly aligned chiral molecules in the chiral liquid crystal media and developed the DQ-SERF (double quantum selective refocusing) experiment which does not utilize the spin state selection but provided unraveling of the overlapped peaks of the selectively excited methyl group proton resonances [24]. The advantages of the DQ-SERF experiment over SERF experiment have been extensively discussed. We have also pointed out that the SERF experiment does not require a biselective pulse and demonstrated that it can also be exploited for the determination of the long distance couplings in the direct dimension. All these methodologies exploit proton–proton dipolar couplings for enantiomeric discrimination.

The chemical shift anisotropy ($\Delta\sigma_i$) of proton is another spectral parameter which has not been utilized exclusively for chiral visualization. The magnitudes of $\Delta\sigma_i$ of protons are known to be very small and are within a few ppm, even in thermotropic liquid crystals where the orientational parameters are several orders of magnitude larger than in chiral liquid crystal. There are exceptional cases like CH_3F and C_2H_2 where the proton chemical shift anisotropies could be significant [25]. However, in general, it is imperative that the $\Delta\sigma_i$ of protons is negligibly smaller in chiral liquid crystals, indicating the reason for not utilizing this as a parameter for enantiomeric discrimination.

In our recent work on spin selective and non-selective excitation of multiple quantum, we have discussed the differences in the spin dynamics in both the situations, reported the theoretical understanding of the spin dynamics using product operator formalism. The study also demonstrated the applicability of spin selective excitation not only for spectral simplification but also for the determination of the relative signs and magnitudes of the scalar couplings [26]. This difference in the spin dynamics inspired us to extend the idea of non-selective excitation for complete unraveling of the optical enantiomers in the present study. The non-selective excitation of homonuclear highest quantum of all the coupled protons results in their simultaneous flipping, providing a singlet for each enantiomer at the sum of their anisotropic chemical shift values in the MQ dimension. In the higher quantum dimension the cumulative addition of anisotropic chemical shifts of each enantiomer provides a sizeable differential value of $\Delta\sigma_i$ between them enabling the complete unraveling. Since the basic requirement is the coupling among all the protons, we are aware of the fact that this methodology is applicable to small molecules. The selective detection of the particular order of the quantum is achieved by employing the gradients. The application and the limitation of the experimental methodology have been demonstrated on the chosen test molecules, each having a chiral centre, viz. (±)-2-chloropropanoic acid, (±)-3-butyn-2-ol, and the mixture of structural isomers of (±)-1-chloro-2-propanol and (±)-2-chloro-1-propanol aligned in the chiral liquid crystal poly(γ-benzyl-L-glutamate) (PBLG).

2. Experimental confirmation

The samples were purchased from Sigma and used without further purification. The racemic structures of these molecules are given in Fig. 1. The samples were prepared by the method described in the literature [11,22]. For the oriented (±)-2-chloropropanoic acid sample, 50 mg of the

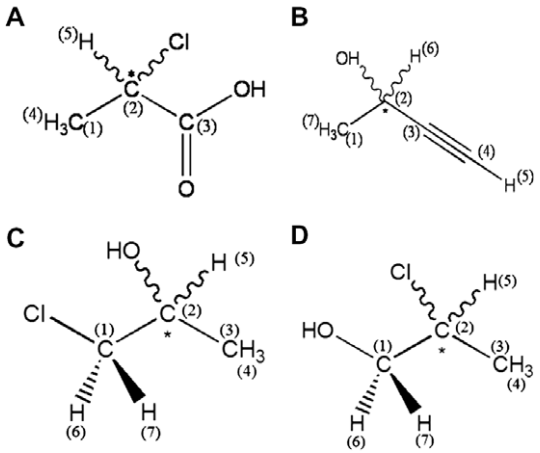

Fig. 1. (A–D) The racemic structures and the numbering of interacting spins in (*R*/*S*)-2-chloropropanoic acid, (*R*/*S*)-3-butyn-2-ol, (*R*/*S*)-1-chloro-2-propanol and (*R*/*S*)-2-chloro-1-propanol, respectively.

racemic sample, 80 mg of PBLG (with DP 782) and 300 mg of $CDCl_3$ were taken. For the oriented (±)-3-butyn-2-ol, 85 mg of PBLG (with DP 782), 59 mg of the sample and 450 mg of $CDCl_3$ were taken. For the oriented mixture (75:25) of isomers (±)-1-chloro-2-propanol and (±)-2-chloro-1-propanol, 110.0 mg of the sample, 105.0 mg of PBLG (with DP 562)and 370.0 mg of $CDCl_3$ were taken. The samples were sealed in a 5 mm NMR tube to avoid the evaporation of the solvent and then centrifuged back and forth for several hours till the visually homogeneous phase was obtained. The orientation of the sample was investigated by monitoring the ^2H doublet separation of $CDCl_3$. The temperature was maintained at 300, 300.0 and 300 K for (±)-2-chloropropanoic acid, (±)-3-butyn-2-ol and the mixture of isomers (±)-1-chloro-2-propanol and (±)-2-chloro-1-propanol, respectively, using Bruker BVT 3000 temperature controller unit of the Bruker DRX-500 NMR spectrometer. The one-dimensional proton spectra of all the molecules are given in Fig. 2.

For the two-dimensional experiment correlating the homonuclear highest quantum coherence to its SQ coherence, the three pulse multiple quantum sequence was employed [27]. In the indirect dimension (t_1 dimension) the highest quantum coherence of all the coupled protons was excited, the magnetization was then converted back to SQ coherence for detection in the direct dimension (t_2 dimension). All the pulses were non-selective and thus there was simultaneous excitation of all the coupled protons. The amplitude of an excited coherence is dependent on the coupling constants. The couplings among the protons are different in each enantiomer. Therefore, the optimization of the τ delay between the first and the second 90° pulses is very important to get a maximum anti phase magnetization. A series of two-dimensional experiments were, therefore, carried out to optimize the τ delay. The intensity of the spectrum for the first t_1 incremental delay corresponding to each enantiomer was monitored as a function of τ delay. The delay which provided maximum and comparable signal intensities for both enantiomers was chosen. This also implies that MQ excitation is non-uniform and the experiment cannot be employed for the quantitative measure of enantiomeric excess. The extensive discussion on the optimization of τ delay, the spectra with different τ delay and the problems and prospects of measuring enantiomeric excess using multiple quantum methodology have already been reported in our earlier work [24].

For the 2D experiment in (±)-2-chloropropanoic acid, correlating homonuclear fourth quantum (4Q) coherence of protons to its SQ coherence, a dataset consisting of 4096 and 1024 points in F_2 (SQ) and F_1 (4Q) dimensions, respectively, was chosen. Spectral widths of 2155 and 2500 Hz were chosen in the direct and indirect dimensions, respectively. The number of accumulations was two for each t_1 increment. The optimized τ delay was 20.8 ms. Relaxation delay used was 2.5 s. The time domain data was processed by zero filling to 8192 and 2048 points in t_2 and t_1 dimensions, respectively, with a sine bell window function for enhancing the resolution and to minimize the overlap of contours. The spectrum was displayed in the magnitude mode with the digital resolution was 0.26 and 1.2 Hz in the direct and indirect dimensions, respectively.

In (±)-3-butyn-2-ol, for the 2D experiment correlating homonuclear fifth quantum (5Q) coherence of protons to its SQ coherence, a dataset consisting of 4096 and 1400

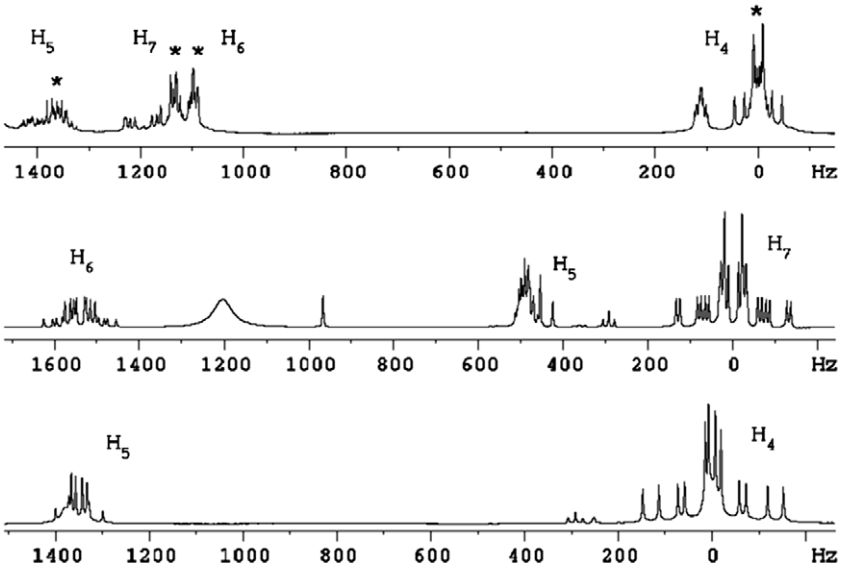

Fig. 2. Bottom trace: 500 MHz one-dimensional ^1H spectrum of (*R*/*S*)-2-chloropropanoic acid; middle trace: 500 MHz one-dimensional ^1H spectrum of (*R*/*S*)-3-butyn-2-ol and top trace: 500 MHz one-dimensional ^1H spectrum of the isomeric mixture (75:25) of (*R*/*S*)-1-chloro-2-propanol and (*R*/*S*)-2-chloro-1-propanol, respectively. The groups of resonances marked * in the top trace are the resonances from one isomer and the unmarked groups of resonances correspond to another isomer. The assignments to different non-equivalent protons are from the literature [3,21,28].

points in F_2 and F_1 dimensions, respectively, was chosen. Spectral widths of 2111.0 and 3750.0 Hz were chosen in the direct and indirect dimensions, respectively. The number of accumulations was four for each t_1 increment. Relaxation delay used was 4 s. The optimized τ delay was 6.25 ms. The time domain data was processed by zero filling to 8192 and 4096 points in t_2 and t_1 dimensions, respectively, with the use of sine bell window function. The spectrum was displayed in magnitude mode with a digital resolution of 0.25 and 0.92 Hz in the direct and indirect dimensions, respectively.

For the mixture of isomers (±)-1-chloro-2-propanol and (±)-2-chloro-1-propanol the 2D experiment correlating homonuclear sixth quantum (6Q) coherence of protons to its SQ coherence was carried out with a dataset consisting of 8192 and 1024 points in F_2 and F_1 dimensions, respectively. Spectral widths of 3788.0 and 11400.0 Hz were chosen in the direct and indirect dimensions, respectively. The number of accumulations was 4 for each t_1 increment. Relaxation delay used was 5 s. The optimized τ delay was 33 ms. The time domain data was processed by zero filling to 16,384 and 2048 points in t_2 and t_1 dimensions, respectively, with the use of sine bell window function. The spectrum was displayed in magnitude mode with a digital resolution of 0.23 and 5.5 Hz in the direct and indirect dimensions, respectively.

3. Multiple quantum coherence

The MQ NMR and its applications have been reviewed in detail [29,30]. MQ coherence is a coherent superposition of states for which the total spin magnetic quantum number is other than ±1. Spins which undergoes a transition between the two states concerned are called active spins in the coherence and all the remaining spins are said to be passive. The properties of the coherence depend both on its order and on the properties of the active spins and their interactions with the passive spins. The group of active spins can be regarded as a super spin and the remaining passive spins as spectator spins. As the size of the super spin increases, the number of spectator spins decreases and consequently the multiplet structure of the coherence will become simpler. The number of allowed transitions for the 0th and the mth quantum order of N interacting non-equivalent half integer spins are given by;

$$Z_0 = 1/2[{}^{2N}C_N - 2^N] \quad (1)$$

$$Z_m = 2N!/(N-m)!(N+m)! \quad (2)$$

where Z_0 refers to zero quantum (ZQ) and Z_m refers to mth quanta for $m > 1$.

The precessional frequency of any higher quantum order is given by

$$\Omega_{HQ} = \sum_I \Delta m_I \omega_I \quad (3)$$

where ω_{HQ} is the higher quantum precession frequency, Δm_I is the change in the quantum number of the spin I. As an example in a two spin system, for the zero quantum coherence, the effect of a spin undergoing the transition from $|\alpha\rangle$ state to $|\beta\rangle$ state is canceled by the transition from $|\beta\rangle$ state to $|\alpha\rangle$ state, the spins precess at the difference of their chemical shifts. However, for the corresponding double quantum coherence, the spins flip from the state $|\alpha\alpha\rangle$ to the state $|\beta\beta\rangle$ or vice versa. Hence the spins precess at the sum of their chemical shifts. Similarly, in the Nth quantum coherence of N coupled spin system, all the spins flip simultaneously from the state $|\alpha\rangle$ to the state $|\beta\rangle$ or vice versa. Thus the highest quantum spectrum provides information only on the sum of all the chemical shifts. The scalar and the dipolar fields do not influence the spectrum. When the spatially dependent field inhomogeneity, $\Delta B_0(r)$, is also taken into account, the precessional frequency becomes;

$$\omega_{HQ} = \sum \Delta m_I(\omega_I + \gamma_I \Delta B_0(r)) \quad (4)$$

This equation implies that the sensitivity of the precessional frequency of any higher quantum coherence is proportional to its order. Thus mth quantum order broadens the signal "m" times due to B_0 field inhomogeneity. One method is to apply a non-selective 180° pulse in the middle of the t_1 dimension which refocuses the chemical shifts and removes the contributions from the field inhomogeneity [29]. However, this cannot be implemented in the present work as our focus is to exploit the chemical shift anisotropy. The zero quantum coherence is, however, insensitive to the field inhomogeneity.

4. Results and discussion

Assignments of protons to different groups and for all the chosen molecules are available in the literature [4,21,28] and are also marked in the corresponding one-dimensional spectrum. Since the systems are very weakly ordered and the small change in the experimental conditions do not drastically alter the spectral pattern the earlier assignments of resonances to R and S enantiomers were taken.

In (±)-2-chloropropanoic acid, the OH proton signal is excessively broadened and does not shown any coupling with the remaining protons. Hence the coupled protons form a spin system of the type A_3X. The first order analysis of the spectrum is straightforward. The methyl protons are split into a 1:2:1 triplet due to residual proton–proton dipolar couplings among the magnetically equivalent protons. The separation between two adjacent transitions corresponds to ${}^nT_{HH}$, where superscript n refers to protons that are n bonds away. Thus for the methyl triplet, the adjacent transitions provide ${}^2T_{HH}$ ($3D_{HH}$). Each component of the triplet is further split into a doublet of equal intensity due to coupling with methine proton. Similarly, the

methine proton is a quartet due to its coupling with methyl protons.

In (±)-3-butyn-2-ol also the OH resonance is broadened and do not display any coupling to other protons. However, all the remaining protons are coupled among themselves. Therefore, the spin system is of the type A_3MX, where A_3 corresponds to methyl protons, M and X corresponds to protons of methine and acetylenic groups, respectively. The one-dimensional ^1H spectrum has well resolved peaks for the CH_3 and two CH groups. The CH_3 group gives a triplet due to dipolar coupling among the protons, each component of this triplet is further split into the doublet of a doublet from the methine and acetylenic protons. Thus it displays 12 transitions corresponding to four A_3 sub spectra. Similarly each of the methine and acetylenic protons splits into a quartet due to CH_3 group and each component of the quartet is split into a doublet from the remaining single proton.

In the isomeric mixture of (±)-1-chloro-2-propanol and (±)-2-chloro-1-propanol, all the groups of proton resonances are well separated. The OH resonances of both these molecules overlap and resonate at the lower field and do not couple to remaining protons of the molecules. Two methylene protons are diastereotopic and are chemically inequivalent. Therefore, the coupled protons of each component of the mixture form a spin system of the type A_3MNX. The methyl group of each component provides triplet due to coupling among methyl protons which are further split into doublet of doublet of doublet due to two methylene and the methine protons. Likewise the resonances of each of the two methylene and the methine proton are split into doublet of doublet of a quartet.

With well resolved and isolated peaks for different groups of protons the first order analyses of the ^1H spectra of (±)-2-chloropropanoic acid and (±)-3-butyn-2-ol are straightforward. However, the prerequisite is to identify the transitions for each enantiomer. In the isomeric mixture of (±)-1-chloro-2-propanol and (±)-2-chloro-1-propanol also the resonances for different groups of protons are well isolated but the resolution in this case is relatively poor. Therefore, we detected the homonuclear highest quantum coherence of all the coupled spins in these molecules.

The two-dimensional MQ spectra of (±)-2-chloropropanoic acid and (±)-3-butyn-2-ol are shown in Figs. 3 and 4, respectively. The highest possible proton homonuclear MQ orders for the coupled spins in these molecules are 4 and 5, respectively. The differential ordering results in differential chemical shift anisotropies for all the non-equivalent protons of the enantiomers. The differential value between two enantiomers, of the cumulative sum of chemical shift anisotropies of all the coupled protons of each enantiomer, is of measurable magnitude. The higher quantum dimension thus will have two identifiable transitions, each of which corresponds to one of the enantiomers. This is clearly evident from the projection along F_1 dimension, shown in Figs. 3 and 4.

The assignment of peaks to R and S enantiomers in the higher quantum dimension requires the knowledge of the magnitudes and signs of $\Delta\sigma_i$ of inequivalent coupled protons. This is difficult to obtain for the molecules with lower symmetry and this information is not available for the molecules under investigation. However, the cross sections taken along the SQ dimension at the resonating positions of each peak in the MQ dimension pertain to the one-dimensional spectrum of an enantio pure sample. The assignment for R and S enantiomers in the one-dimensional experiment is available [4,21]. With this knowledge and from the cross section taken along SQ dimension, it was possible to assign the peaks to R and S enantiomers in the MQ dimension. The cross section taken along SQ for S enantiomer in (±)-2-chloropropanoic acid and for R enantiomer in (±)-3-butyn-2-ol are plotted below the 2D spectrum in Figs. 3 and 4, respectively. In (±)-2-chloropropanoic acid, all the six peaks of the methyl group and four peaks for the methine proton are clearly separated from the overlapped spectra. Similarly in (±)-3-butyn-2-ol, 12 peaks for the methyl, eight peaks each for methine and acetylinic protons are filtered out. For acetylenic proton, the peak marked * indicates the overlapped peak from the S enantiomer. Thus the experiments clearly demonstrate the unambiguous and complete unraveling of the spectra for each enantiomer from the superimposed spectra.

With the unraveling thus achieved, the first order ananlyses of the spectra (cross sections taken along the SQ dimension) for both the molecules were carried out. The coupling information is determined from the separations $^nT_{HH}$, n (=2, 3) for (±)-2-chloropropanoic acid and n (=2, 3, 5) for (±)-3-butyn-2-ol. The main focus of our study is to develop the methodology. Furthermore, there are extensive studies on these molecules reported in the literature [21,4]. Hence we have reported only the separations and not the magnitudes and signs of the couplings. These separations are;

For (R/S)-2-chloropropanoic acid;

$(^2T_{HH})^R = 59.7$ Hz and $(^3T_{HH})^R = 15.6$ Hz

$(^2T_{HH})^S = 110.3$ Hz and $(^3T_{HH})^S = 25.1$ Hz

For (R/S)-3-butyn-2-ol;

$(^2T_{HH})^R = 103.4$ Hz,

$(^3T_{HH})^R = 49.4$ Hz and $(^5T_{HH})^R = 9.1$ Hz

$(^2T_{HH})^S = 88.4$ Hz, $(^3T_{HH})^S = 32.8$ Hz

and $(^5T_{HH})^S = 9.3$ Hz.

The only other study where the total discrimination could be achieved is by homonuclear total correlation [20].

The present method also suffers from certain limitations. Firstly, it achieves unraveling but the broadening of the spectra of individual R and S enantiomers, due to numerous long and short distance couplings, still persists, secondly to achieve discrimination the difference in the

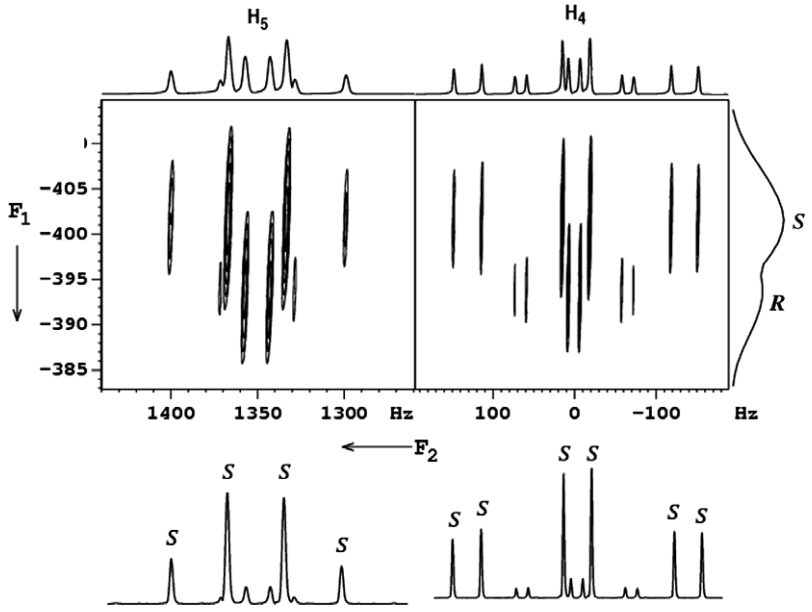

Fig. 3. Five-hundred mega hertz 2D spectrum of (*R*/*S*)-2-chloropropanoic acid, aligned in the chiral liquid crystal PBLG, correlating the 4Q coherence of protons to its SQ coherence along with the corresponding projections. t_1 and t_2 dimensions corresponds to 4Q and SQ detection. Assignment for the enantiomers *R* and *S* marked in 4Q and SQ dimensions is with the knowledge available in the literature [21]. One-dimensional spectrum given below the 2D spectrum is the cross section taken along SQ dimension at the position of *S* enantiomer in the MQ dimension. Due to large spread of the contours, the less intense peaks from *R* enantiomer are also seen.

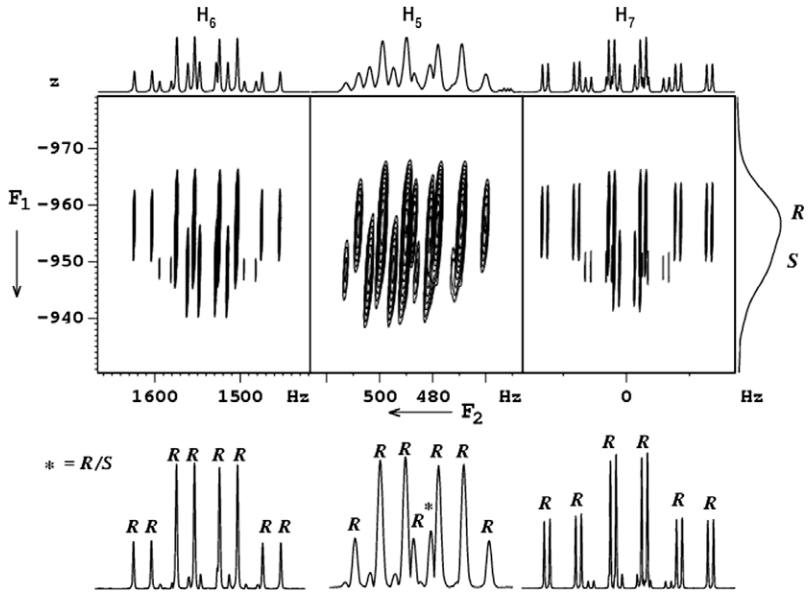

Fig. 4. Five-hundred mega hertz 2D spectrum of (*R*/*S*)-3-butyn-2-ol, aligned in the chiral liquid crystal PBLG, correlating the 5Q coherence of protons with SQ coherence along with the corresponding projections. t_1 and t_2 dimensions corresponds to 5Q and SQ detection. Assignment for the enantiomers *R* and *S* in 5Q and SQ dimensions is with the knowledge available in the literature [3]. One-dimensional spectrum given below the 2D spectrum is the cross section taken along SQ dimension at the position of *R* enantiomer in the 5Q dimension. The peak marked * has also the overlap of a peak from *S* enantiomer. Due to large spread of the contours, the portion of the spectrum from *S* enantiomer is also seen.

cumulative additive values of $\Delta\sigma_i$ should be of measurable magnitude. These two situations hamper the application of this methodology. Analogous situation was clearly evident in the 6Q spectrum of the isomeric mixture of (±)-1-chloro-2-propanol and (±)-2-chloro-1-propanol shown in Fig. 5. The differential value of sum of the anisotropic chemical shifts of each component of the isomeric mixture is 545.0 Hz and these two spectra could be completely unraveled in the 6Q dimension. The conceptual understanding and the applications of spin topology filtering using multiple quantum excitation is well known in the literature [31–33], although, in the present study it is the separation of isomers of identical spin topologies and spin systems (A_3MNX). However, the poor resolution did not permit

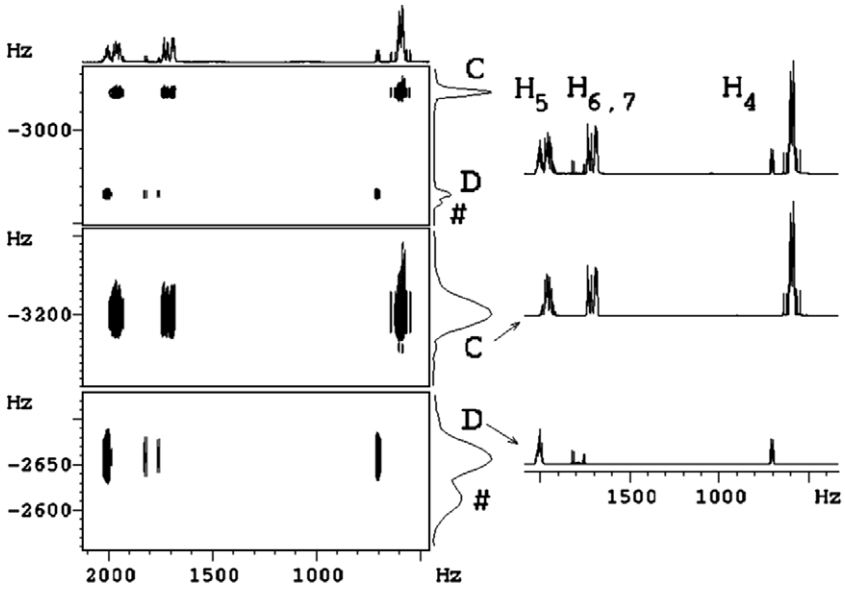

Fig. 5. Five-hundred mega hertz 2D spectrum of the isomeric mixture (75:25) of (±)-1-chloro-2-propanol and (±)-2-chloro-1-propanol aligned in the chiral liquid crystal PBLG, correlating the 6Q coherence of protons with SQ coherence along with the corresponding projections. t_1 and t_2 dimensions corresponds to 6Q and SQ detection. C and D marked in the 6Q dimension correspond to the one-dimensional spectrum of (±)-1-chloro-2-propanol and (±)-2-chloro-1-propanol, respectively. The plot on the right side of 2D matrix (top trace) is the projection taken along F_2 dimension. The MQ spectrum for each isomer is plotted below and are also marked C and D. The cross sections taken along F_2 dimension for the isomers C and D is plotted on the right side and are shown by arrows. The assignments for different protons are taken from the literature [28]. The peak marked # in the MQ dimension is the unknown impurity.

the individual separation of peaks pertaining to *R* and *S* enantiomers.

Another problem in the higher quantum detection is the contributions from the magnetic field inhomogeneity. Due to its linear dependence with the higher quantum order, there is enhanced contour spread. This is the reason for appearance of less intense peaks of other enantiomer in the cross sectional plots given in Figs. 3 and 4. The development of a phase sensitive version of the experiment is another alternative for obtaining high resolution. Our initial results using the phase sensitive version did not improve the resolution significantly. However, this did not preclude us from unraveling the enantiomers and measuring the relative difference in their frequency positions and derive the spectral parameters for the two molecules reported here. The further investigations and methodological developments are essential for; (a) to reduce the contour widths to enable unraveling when the difference in $\Delta\sigma_i$ is very small and (b) for application to molecules with more number of interacting spins. The studies in this direction are in progress.

5. Conclusions

The differential ordering property of enantiomers in chiral liquid crystalline media affects the chemical shift anisotropy differently. The *N*th quantum coherence of *N* coupled spins results in the simultaneous flipping of all the spins at the sum of their chemical shifts. The method is applicable to small molecules where all the protons are coupled among themselves. The differential value between the enantiomers, in the cumulative additive values of chemical shift anisotropies of all the coupled protons of each enantiomer, results in their measurable separation in the higher quantum dimension. The cross sections taken along the SQ dimension at the resonance positions of each enantiomer in the MQ dimension pertains to the one-dimensional enantio pure spectrum. Thus the method not only unambiguously identifies the transitions for each enantiomer but also achieves their complete unraveling. The pulse sequence is easy to implement and the selection of the particular MQ order is achieved by using gradients. The method also provides the separation of the components in the mixture of different molecules. The method has a limitation when the differential sum of $\Delta\sigma_i$ between the enantiomers is immeasurably small and in bigger molecules where all the spins are obviously not coupled.

Acknowledgments

NS gratefully acknowledges the financial support by Department of Science and Technology, New Delhi for the Grant No. SR/S1/PC-13/2004. URP and BB thank Council of Scientific and Industrial Research (CSIR), India, for research fellowship.

References

[1] D. Parker, NMR determination of enantiomeric purity, Chem. Rev. 91 (1991) 1441.

[2] R. Rothchild, NMR methods for determination of enantiomeric excess, Enantiomer 5 (2000) 457–471.
[3] M. Sarfati, P. Lesot, D. Merlet, J. Courtieu, Theoretical and experimental aspects of enantiomeric differentiation using natural abundance multinuclear NMR spectroscopy in chiral polypeptide liquid crystals, Chem. Commun. (2000) 2069–2081.
[4] P. Lesot, D. Merlet, J. Courtieu, J.W. Emsley, T.T. Rantala, J. Jokisaari, Calculation of the molecular ordering parameters of (±)-3-butyn-2-ol dissolved in an organic solution of poly(γ-benzyl-L-glutamate), J. Phys. Chem. A. 101 (1997) 5719–5724.
[5] I. Canet, J. Courtieu, A. Loewenstein, A. Meddour, J.M. Péchiné, Enantiomeric analysis in polypeptide lyotropic liquid crystal by deuterium NMR, J. Am. Chem. Soc. 117 (1995) 6520–6525.
[6] D. Merlet, B. Ancian, W. Smadja, J. Courtieu, P. Lesot, Analysis of natural abundance deuterium NMR spectra of enantiomers in chiral liquid crystals *via* 2D auto-correlation experiments, Chem. Commun. (1998) 2301–2302.
[7] A. Meddour, A. Haudrechy, P. Berdagué, W. Picoul, Y. Langlois, J. Courtieu, Analysis of the diastereoselectivity of a Diels-Alder cycloaddition through ^{2}H NMR in chiral liquid crystals, Tetrahedron Asymm. 7 (1996) 2489–2492.
[8] D. Merlet, M. Sarfati, B. Ancian, J. Courtieu, P. Lesot, Description of natural abundance deuterium 2D NMR experiments in weakly ordered liquid-crystalline solvents using a tailored Cartesian spin-operator formalism, Phys. Chem. Chem. Phys. 2 (2000) 2283–2290.
[9] P. Lesot, D. Merlet, A. Loewenstein, J. Courtieu, Enantiomeric visualisation using proton-decoupled natural abundance deuterium NMR in poly(γ-benzyl-L-glutamate) liquid crystalline solutions, Tetrahedron Asymm. 9 (1998) 1871–1881.
[10] O. Lafon, P. Lesot, D. Merlet, J. Courtieu, Modified z-gradient filtering as a mean to obtain phased deuterium autocorrelation 2D NMR spectra in oriented solvents, J. Magn. Reson. 171 (2004) 135–142.
[11] D. Merlet, B. Ancian, J. Courtieu, P. Lesot, Two-dimensional deuterium NMR spectroscopy of chiral molecules oriented in a polypeptide liquid crystal: applications for the enantiomeric analysis through natural abundance deuterium NMR, J. Am. Chem. Soc. 121 (1999) 5249–5258.
[12] K. Ben Ali, O. Lafon, H. Zimmermann, E. Guittet, P. Lesot, Homo- and heteronuclear 2D NMR approaches to analyse a mixture of deuterated unlike/like stereoisomers using weakly ordering chiral liquid crystals, J. Magn. Reson. 187 (2007) 205–215.
[13] P. Lesot, O. Lafon, J. Courtieu, P. Berdagué, Analysis of the ^{13}C NMR spectra of molecules, chiral by isotopic substitution, dissolved in a chiral oriented environment: towards the absolute assignment of the pro-R/pro-S character of enantiotopic ligands in prochiral molecules, Chem. Eur. J. 10 (2004) 3741–3746.
[14] A. Meddour, P. Berdague, A. Hedli, J. Courtieu, P. Lesot, Proton-decoupled carbon-13 NMR spectroscopy in a lyotropic chiral nematic solvent as an analytical tool for the measurement of the enantiomeric excess, J. Am. Chem. Soc. 119 (1997) 19,4502–19,4508.
[15] V. Madiot, P. Lesot, D. Grée, J. Courtieu, R. Gree, Highly enantioselective propargylic monofluorination established by carbon-13 and fluorine-19 NMR in chiral liquid crystals, Chem. Comm. (2000) 169–170.
[16] M. akubcova, A. Meddour, J.M. Péchiné, A. Baklouti, J. Courtieu, Measurement of the optical purity of fluorinated compounds using proton decoupled ^{19}F NMR spectroscopy in a chiral liquid crystal solvent, J. Fluorine Chem. 86 (1997) 149–153.
[17] J. Farjon, D. Merlet, P. Lesot, J. Courtieu, Enantiomeric excess measurements in weakly oriented chiral liquid crystal solvents through 2D ^{1}H selective refocusing experiments, J. Magn. Reson. 158 (2002) 169–172.
[18] T. Fäcke, S. Berger, SERF, a new method for H,H spin-coupling measurement in organic chemistry, J. Magn. Reson. A 113 (1995) 114–116.
[19] L. Beguin, J. Courtieu, L. Ziani, D. Merlet, Simplification of the ^{1}H NMR spectra of enantiomers dissolved in chiral liquid crystals, combining variable angle sample spinning and selective refocusing experiments, Magn. Reson. Chem. 44 (2006) 1096–1101.
[20] P. Lesot, D. Merlet, J. Courtieu, J.W. Emsley, Discrimination and analysis of the NMR Spectra of enantiomers dissolved in chiral liquid crystal solvents through 2D correlation experiments, Liquid Crystals 21 (1996) 427–435.
[21] J. Farjon, J.P. Baltaze, P. Lesot, D. Merlet, J. Courtieu, Heteronuclear selective refocusing 2D NMR experiments for the spectral analysis of enantiomers in chiral oriented solvents, Magn. Reson. Chem. 42 (2004) 594–599.
[22] L. Ziani, J. Courtieu, D. Merlet, Visualisation of enantiomers via insertion of a BIRD module in X–H correlation experiments in chiral liquid crystal solvent, J. Magn. Reson. 183 (2006) 60–67.
[23] B. Bikash, N. Suryaprakash, Spin state selective detection of single quantum transitions using multiple quantum coherence, simplifying the analysis of complex NMR spectra, J. Phys. Chem. A. 111 (2007) 5211–5217.
[24] B. Bikash, R.P. Uday, N. Suryaprakash, Enantiomeric discrimination by double quantum excited selective refocussing (DQ-SERF) experiment, J. Phys. Chem. B. 111 (2007) 12403–12410.
[25] J. Lounila, J. Jokisaari, Anisotropies in spin–spin coupling constants and chemical shifts as determined from the NMR spectra of molecules oriented by liquid crystal solvents, Prog. NMR Spect. 15 (1982) 249–290.
[26] B. Bikash, N. Suryaprakash, Spin selective multiple quantum NMR for spectral simplification, determination of relative signs and magnitudes of scalar couplings by spin state selection, J. Chem. Phys. 127 (2007) 214510.
[27] A. Bax, R. Freeman, T.A. Frenkiel, M.H. Levitt, Assignment of ^{13}C spectra via double quantum coherence, J. Magn. Reson. 43 (1981) 478–483.
[28] V.M. Marathias, I. Goljer, A.C. Bach II, Simultaneous determination of ^{1}H–^{1}H and ^{1}H–^{13}C residual dipolar couplings in a chiral liquid crystal solvent using a natural abundance HSQC experiment, Magn. Reson. Chem. 43 (2005) 512–519.
[29] T.J. Norwood, Multiple quantum NMR methods, Prog. NMR Spect. 24 (1992) 295–375.
[30] G. Bodenhausen, Multiple quantum NMR, Prog. NMR Spect. 14 (1981) 137–173.
[31] A.J. Shaka, R. Freeman, Simplification of NMR spectra by filtration through multiple quantum coherence, J. Magn. Reson. 53 (1983) 169–173.
[32] M.H. Levitt, R.R. Ernst, Spin-pattern recognition in high-resolution proton NMR spectroscopy, Chem. Phys. Lett. 100 (1983) 119–123.
[33] M.H. Levitt, R.R. Ernst, Multiple-quantum excitation and spin topology filtration in high-resolution NMR, J. Chem. Phys. 83 (1985) 3297–3310.